Rapid Test of Pneumonia Cells: An Alternative Simple Application

Article · October 2022

CITATIONS
0

READS
2

4 authors, including:

Haris Imam Karim Fathurrahman
Ahmad Dahlan University
7 PUBLICATIONS **37** CITATIONS
SEE PROFILE

Riky Dp
Ahmad Dahlan University
21 PUBLICATIONS **60** CITATIONS
SEE PROFILE

Ahmad Azhari
Ahmad Dahlan University
27 PUBLICATIONS **64** CITATIONS
SEE PROFILE

Rapid Test of Pneumonia Cells: An Alternative Simple Application

FATHURRAHMAN Haris Imam Karim[1], PURIYANTO Riky Dwi[1], KAMILAH Farhah[2]
AZHARI Ahmad[3]

[1] Universitas Ahmad Dahlan, Indonesia,
Department of Electrical Engineering, Faculty of Industrial Technology,
Jl. Kapas No.9, Semaki, Kec. Umbulharjo, 55166 Yogyakarta, Indonesia, E-Mail: haris.fathurahman@te.uad.ac.id, rikydp@ee.uad.ac.id

[2] University Muhammadiyah Yogyakarta, Indonesia,
School of Nursing, Faculty of Medicine and Nursing,
Jl. Brawijaya, Kasihan, Bantul,
55183 Yogyakarta, Indonesia, E-Mail: farhahkamilah28@gmail.com

[3] Universitas Ahmad Dahlan, Indonesia,
Department of Informatics, Faculty of Industrial Technology,
Jl. Kapas No.9, Semaki, Kec. Umbulharjo, 55166 Yogyakarta, Indonesia, E-Mail: ahmad.azhari@tif.uad.ac.id

Abstract *– In this pandemic period, pneumonia is often found in various cases. In many cases, COVID-19 has an adverse effect on people with pneumonia. Early detection of pneumonia can help health institutions map pneumonia in the community. However, pneumonia detection still uses conventional methods and takes a long time. This study detects pneumonia bacteria consisting of Acinetobacter baumannii and Pseudomonas aeruginosa. This study uses the DIBaS database, which consists of several bacterial images. This database is used to compare two classes, namely pneumonia and non-pneumonia. Detection is carried out using an artificial intelligence approach using the DenseNet121 and DenseNet169 methods. This study also uses the Genetic Algorithm optimization method to increase the accuracy of detecting pneumonia bacterial cells. The Genetic Algorithm provides random values for the last two DenseNet121 and DenseNet169 training layers. As a result, the accuracy of the DenseNet121 and DenseNet169 methods reached 95% and 96.7%, respectively. The optimization method intervention gave an increase of 5.2% and 3.4% over the original method, respectively. The best model results from this method are used as a reference model in making applications for the rapid detection of pneumonia with an average speed of accuracy reaching 4.25s. This computer-based application provides promising results for the future to be applied to the broader community.*

Keywords: *Artificial Intelligence; Computer-based Application; Genetic Algorithm; Pneumonia*

I. INTRODUCTION

The pandemic era in 2020-2021 impacts the increasing trend of pneumonia. Covid-19, a disease that attacks the respiratory system, affects the emergence of pneumonia. Pneumonia is caused by several bacterial infections that attack the respiratory system. There are two bacteria found in patients with pneumonia, including Acinetobacter baumannii and Pseudomonas aeruginosa. Acinetobacter baumannii and Pseudomonas aeruginosa are the most common nosocomial pathogens, producing infections in the bloodstream, urinary system, wounds, and burns [1], [2], [3]. These two bacteria are frequently discovered in hospitals, particularly in intensive care units (ICU). They can adhere to medical devices (including systems used for mechanical ventilation) and survive for up to 33 days on dry surfaces, so patients with long hospital stays are at a higher risk of exposure to these [1]. These bacteria are gram-negative bacilli that are aerobic, pleomorphic, and non-motile [4]. These bacteria specifically target moist tissues such as mucous membranes or exposed areas of skin, either by accident or injury, and can quickly enter the body through open wounds, intravascular catheters, and mechanical ventilators [4], [5].

Acinetobacter baumannii and Pseudomonas aeruginosa are the most common pathogens responsible for ventilator-associated pneumonia (VAP) and bloodstream infections, with mortality rates ranging from 5% in general hospital wards to 54% in intensive care units (ICU) [1], [6], [7]. In an observational study conducted across Europe, Acinetobacter was the third most prevalent bacterium responsible for VAP in an observational study conducted across Europe, behind

Staphylococcus aureus and Pseudomonas aeruginosa [8]. In an evaluation of 27 intensive care units in nine European countries, Pseudomonas aeruginosa was responsible for 26% of early VAP (<5 days) and 55% of late sVAP (≥5 days). In contrast, Acinetobacter baumannii was responsible for 16% of early VAP (<5 days) and 55% of late sVAP (≥5 days) [9]. An increased risk of VAP is enhanced by older age, prolonged hospitalization, prolonged mechanical ventilation, and past antibiotic usage [10]. VAP caused by MDR A. baumannii and P. aeruginosa continues to be a significant cause of high mortality in critically ill patients. While A. baumannii contributes for 8%–14% of VAP in the United States and Europe, this pathogen is linked with significantly higher rates (19% to >50%) in Asia, Latin America, and several Middle Eastern nations [2]. According to a recent meta-analysis including 29 countries, the MDR phenotype was present in close to 80% of A. baumannii isolates, causing hospital-acquired pneumonia and VAP. The largest incidence is seen in Central America, Latin America, and the Caribbean, while the lowest frequency is found in East Asia [8]. Meanwhile, P. aeruginosa MDR infection frequency has grown over the previous several decades and is currently between 15% and 30% in some areas [11]. P. aeruginosa exhibited combined resistance, with 13.7% of isolates resistant to at least three antimicrobial groups and 5.5% resistant to all five antimicrobial groups under observation [12].

Infections with A. baumanni and P. aeruginosa were also detected in infected patients with COVID-19 [13], [14], [15]. Due to airway dysfunction, patients with severe COVID-19 typically require endotracheal intubation and mechanical breathing. For instance, two-thirds of COVID-19 patients who require critical care require mechanical breathing within 24 hours of admission, followed by rapid transfer to an intensive care unit (ICU). Patients undergoing tracheal intubation and mechanical ventilation have a higher risk of contracting bacterial ICU pneumonia [16], [17]. Nineteen COVID-19 patients were discovered to be positive for bacteria, including seventeen species of Acinetobacter baumannii (90%) and two forms of Staphylococcus aureus (10%) and 18 of them died [4]. Pseudomonas aeruginosa infection was detected in 12% of COVID-19 patients in a survey of 17 studies [18]. Another research indicated that 38 COVID-19 patients experienced bacterial infections, with P. aeruginosa being the most frequently identified pathogen [19]. Acinetobacter baumannii and Pseudomonas aeruginosa have been identified as the causal pathogens of VAP in COVID-19-infected people [20]. Deng et al. (2020) [21] researched the electronic medical records of 25 patients diagnosed with COVID-19 at Wuhan University's Renmin Hospital and discovered that bacterial pneumonia might be connected with the mortality of patients infected with the new coronavirus. Similarly, Wang et al. (2020) [22] demonstrated that procalcitonin levels, a hallmark of bacterial infection, were approximately fourfold greater in patients who died from COVID-19 infection than those who recovered.

Acinetobacter baummanii is also suspected of being a significant cause of bloodstream infections in clinical settings, with intravenous or respiratory catheters being a common route of infection [1], [23]–[25]. The mortality rate from A. baumannii bloodstream infections is nearly 40% [6]. Other infections caused by A. baumanni and P. aeruginosa include nosocomial meningitis. P. aeruginosa causes meningitis with a high mortality rate of 33%, particularly in patients who do not withdraw their catheters and do not employ the intrathecal route of administration [26]. Additionally, some research indicates that mortality from P. aeruginosa meningitis varies between 20% and 80% [27]. Meanwhile, Acinetobacter baummanii is an increasing hazard in neurosurgical critical care units, with a mortality rate reaching 70%, particularly in patients with ventriculostomy tubes or cerebrospinal fistulas, which are receiving postoperative antibiotic treatment [6], [28]. Additionally, these bacteria have been identified in the skin and soft tissues of patients who have sustained severe burns, wounds, or trauma, such as troops injured during military operations or victims of natural disasters [29]. Afghanistan and Iraq continue to be the primary geographic areas where A. baumannii is isolated from wounds or soft tissues, particularly following severe injury [30]. Those with A. baumannii infection had more severe burns and comorbidities, more extended hospital stays, and a greater death rate than patients without infection [31]. Additionally, 26 possible biomarkers for early sepsis linked with P. aeruginosa infection in thermal injury have been found in another research [32].

Acinetobacter baummanii and Pseudomonas aeruginosa can also cause urinary tract infections, which can progress to pyelonephritis in people who have catheters [33]. Infections of the urinary tract are usually caused by Escherichia coli bacteria, accounting for up to 80% of cases, whereas Pseudomonas aeruginosa is identified less frequently (7–15%) [34]. However, urinary tract infections were more frequently caused by uropathogenic (by isolation site) P. aeruginosa, which had a higher incidence of antibiotic resistance and a larger proclivity for biofilm formation on medical devices than E. coli. Additionally, another study found that one in every five strains of A. baumannii causes urinary tract infections, particularly when urinary catheters are inserted, accounting for 1.6% of urinary tract infections acquired in the intensive care unit [35]. Additionally, research conducted in Jakarta revealed a strong association between the use of urinary catheters and A. baumannii infection in patients treated in intensive care units [36]. These bacterial infections exacerbate the patient's condition, particularly in patients who have had long-term nurses in the hospital. Periodic monitoring and maintenance of the environment,

equipment, and patients is necessary to avoid bacterial development, particularly in patients who rely on supportive systems such as catheters and ventilators.

Based on the description of the two pathogens, there have been several studies discussing the detection of pneumonia in recent years. Based [37]–[39], describes and uses a method with an artificial intelligence approach to classify pneumonia based on X-Ray. In line with this, M. La Salvia *et al.* [40] use an Artificial Intelligence approach to classifying pneumonia based on computed tomography (CT) scans and chest X-rays data. Some of these research studies generally detect pneumonia disease using patient X-Ray data. The detection and classification of pneumonia disease are still in the X-Rays photo stage and have not yet reached a more specific stage, namely cells.

Artificial intelligence was employed as an auxiliary tool in all of these classification methods. In recent years, artificial intelligence has seen tremendous progress as an implementation in mobile [41]–[43] and computer applications [44], [45]. Artificial intelligence models may be used in the application to categorize illness [46]–[49], stuffs [44], [50], [51], and agriculture [52]–[54]. Existence of artificial intelligence-based applications can be used to anticipate disease pathogens such as the two pneumonia pathogens.

Therefore, a detection method is needed that can be used to classify pneumonia specifically against two bacterial cells, namely Acinetobacter baummanii and Pseudomonas aeruginosa. These two bacterial cells can be classified as pneumonia found in the patient. This research aims to create a fast and easy method based on artificial intelligence approaches to detect these bacteria and organize them into two classes: pneumonia and non-pneumonia.

II. MATERIAL AND METHODS

A. *Dataset augmentation and selecting the pneumonia class*

Data used in this study using bacterial cell image data from B. Zieliński *et al.* [55] research. The dataset consists of 660 image data from several bacteria cell species. In this study, the dataset used is only two classes of bacteria (Acinetobacter baummanii and Pseudomonas aeruginosa) to classify pneumonia diseases. The image data from these classes are augmented flip 90 degrees, 180 degrees, and 270 degrees. So, the total number of images from the pneumonia class is 160 images. On the other hand, the non-pneumonia dataset images use several bacterial pictures with a unique contrast and a highly different color from the pneumonia dataset.

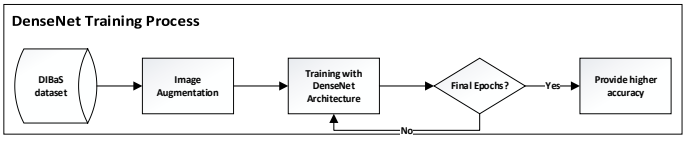

Fig. 1: DenseNet training process

B. *DenseNet and Genetic Algorithm Method*

CNN, or Convolutional Neural Network, is a type of sophisticated artificial intelligence. Convolutional Layers, Relu Layers, Pooling, and Fully Connected Layers are among the layers of CNN. The computation and functioning of the convolution layers based on Mao [56], [57] may be demonstrated mathematically in formula (1). Formulas (2)-(3) can be employed in the Relu and Pooling general formula for sharpening learning results.

$$u_\ell^{fg} = \sum_{g=1}^{F_{\ell-1}} u_l^{fg} = \sum_{g=0}^{F_{\ell-1}} h_l^{fg} * x_{\ell-1}^{g} \quad (1)$$

$$f(x) = \max(x,0) \quad (2)$$

$$[v_\ell^f]_n = p\ell([u_\ell^f]_{n_\ell}) \quad (3)$$

Where x is an input neuron and u_ℓ^{fg} is associated with each of the previous layer features $x_{\ell-1}^{g}$.

The DenseNet technique is one of CNN's approaches. The DenseNet architecture has several Dense Block layers. The final layer is the output network at the end of the DenseNet architecture. This network output has two fully-connected layer parameters that can be set and variable adjusted. As in Figure 1, the training process in DenseNet uses the DIBaS database. This training process will stop when it meets the maximum epoch value. At the end of the training process, an accuracy value is generated for specific fully-connected layer parameters. This parameter will be used as input optimization for the Genetic Algorithm (GA) [41]. The overall learning process of the Genetic Algorithm approach can be seen briefly in Figure 2. Initially, these parameters were assigned a random value by GA. The genetic algorithm processes and performs crossovers and mutations with this random value to obtain exceptional accuracy based on predetermined parameters. GA performs calculations and identifies the best accuracy of each generation. The generation used is four generations in the entire GA operation. GA algorithm, which is a composition of the best parameters, has the highest accuracy at the end of the generation process. The accuracy and loss of the DenseNet algorithm based on W. L. Mao [56] can be calculated using the formula (1)-(2).

$$Accuracy = \frac{Number\ of\ correct\ prediction}{Total\ number\ of\ images} \quad (4)$$

$$Loss = \frac{1}{N}\sum_{n=1}^{N}\sum_{i=1}^{K}(Images\ train - Images\ test)^2 \quad (5)$$

This review will be used as the best parameter solution for the output of GA operations while saving the model

in Keras format. All training experiments were implemented in Python 3.7.1, using Keras to train DenseNet and GA models on GeForce RTX 2080 Super, and performed on an Intel Core i7-9700F with Windows 10.

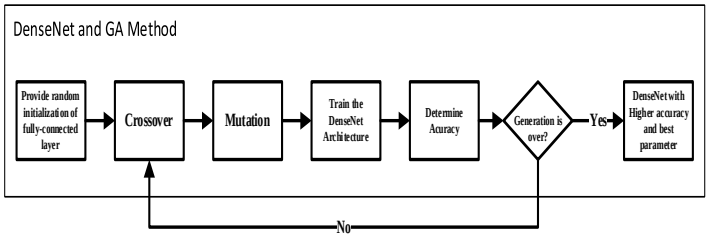

Fig. 2: DenseNet and Genetic Algorithm combination method

C. *Rapid test application development*

The process of making computer-based applications begins by using the best model from the learning outcomes of DenseNet and GA. The model is used as a cell-test reference model—rapid test application development using the C# programming language, directly affiliated with Visual Studio. The Graphical User Interface in this application uses concise and straightforward principles. According to this principle, it is hoped to make it easier for users to directly detect cells obtained through the computer's internal storage. Keras C# support this application platform in visual studio.

III. RESULTS AND DISCUSSION

In this study, DenseNet architecture training was carried out through 4 criteria. The first criterion uses the original DenseNet121 with the same parameters without any changes. In line with this, the second criterion also uses the same parameters but changes the architecture type to DenseNet169. On the other hand, both DenseNet121 and DenseNet169 architectures are used for the third and fourth criteria but modified by adding a Genetic Algorithm.

TABLE I
RANDOM VALUE AND ACTUAL VALUE

Layer	Parameter	Number code in GA	The real value in DenseNet
Fully-connected layer 1	Neuron number	[0, 1, 2, 3, 4, 5, 6, 7, 8, 9]	[1, 128, 256, 384, 512, 640, 768, 896, 1024, 2048]
	Dropout rate	[0, 1, 2, 3, 4, 5]	[0%. 10%, 20%, 30%, 40%, 50%]
Fully-connected layer 2	Neuron number	[0, 1, 2, 3, 4, 5, 6, 7, 8, 9]	[1, 128, 256, 384, 512, 640, 768, 896, 1024, 2048]
	Dropout rate	[0, 1, 2, 3, 4, 5]	[0%. 10%, 20%, 30%, 40%, 50%]

The genetic algorithm has the task of providing a random value that is used to fill in the parameters of the fully-connected layer in DenseNet. In the early stages of the genetic algorithm, this study uses several criteria as a reference to assign a random value to DenseNet. Table 1 describes the number of addresses and the values contained in the random values.

Several accuracy results were obtained based on the results of trials and training data using the provided parameters. The original DenseNet learning using DenseNet121 and DenseNet 169 had an accuracy rate of 95% and 96.7%, respectively. Meanwhile, using a genetic optimization algorithm produces an accuracy of 100% for both. This means that optimization using the Genetic Algorithm increases the accuracy of pneumonia cell detection by 5.2% and 3.4%, respectively. The graphic data of the four accuracies can be seen in Figure 3. Figures 3(b) and 3(d) can also be interpreted as the optimization carried out by the Genetic Algorithm to have a graph that tends to be stable and without significant spikes.

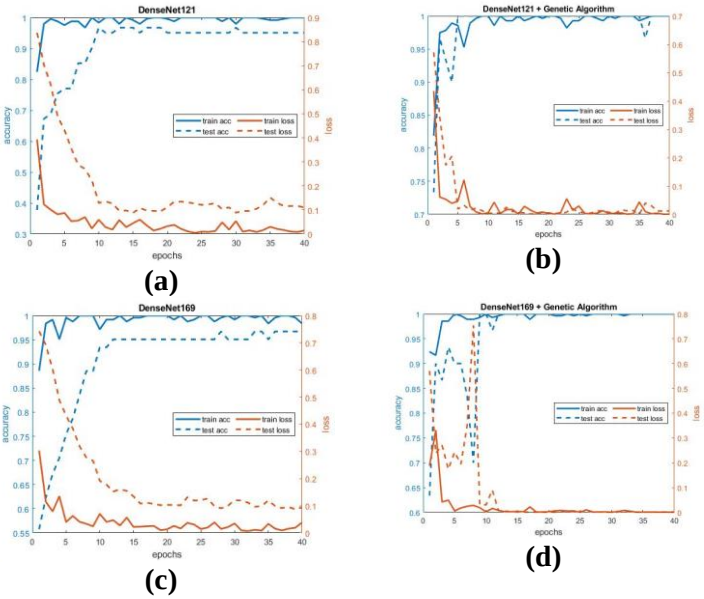

Fig. 3: Results of Accuracy and Loss of Each Method

The best results from each generation in the Genetic Algorithm become the reference model to be saved and converted into Keras model format. The best value data from each DenseNet architecture optimized by a Genetic Algorithm can be seen in Table 2. The saved model will be used as a reference model for applying C# rapid detection of pneumonia.

TABLE II
ACCURACY AND BEST VALUE OF THE PARAMETER.

Method	Accuracy (%)	Parameter			
		FC layer 1		FC layer 2	
		Neuron number	Dropout rate (%)	Neuron number	Dropout rate (%)
DenseNet121	95%	-	-	-	-
DenseNet169	96,7%	-	-	-	-
DenseNet121 + GA	100%	896	0	128	40

DenseNet169 + GA	100%	1024	0	640	50

The working process of the pneumonia rapid detection application uses a simple and practical principle. With this computer-based application, users use laboratory image sample data to detect whether they are included in pneumonia or non-pneumonia bacteria samples. How it works in detail can be seen in Figure 4.

TABLE III
CONFUSION MATRIX DENSENET169

Actual	**Pneumonia**	**Non-pneumonia**
Pneumonia	14	0
Non-pneumonia	0	16

The confusion matrix is used to validate the accuracy of categorization data. Table 3 shows that the validation data for the sample DenseNet169 model with Genetic Algorithm optimization contains no classification mistakes. This is reflected with a value of 0 for each criterion's misclassification. In Figure 4, the initial process is to select an image from the directory, then press predict. After the button is pressed, the best model from the previous training results is used as a reference model to detect the class. Figure 5a illustrates the application display when detecting pneumonia bacterial cells. While Figure 5(b) describes the detection outside the pneumonia class. In less than 10s, the prediction result will appear on the computer-based application screen—however, the prediction time decreases after the first image detection to an average of 4,25s. The detection speed is getting faster because the first execution needs to run the reference model. The actual data of prediction time using rapid test pneumonia application can be seen in Table 4.

TABLE IV
TIME PREDICTIONS

Number	**Time**
Image 01	9s (Initialization and prediction)
Image 02	4s (Prediction)
:	:
:	:
Image 20	4s (Prediction)
Average detection	**4,25s**

When compared to other implementation approaches, the speed of image detection in this computer-based application is faster. According to DiFilippo's research [45], the detection speed is 2.45s quicker. However, the detection time is slower than picture detection utilizing artificial intelligence that does not involve computer applications [58].

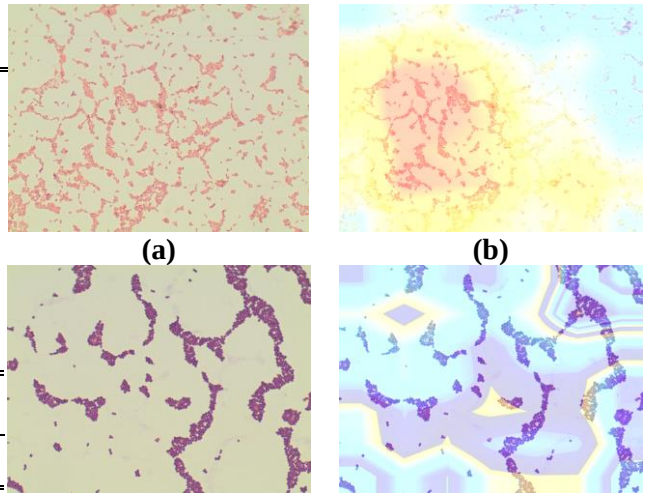

Fig. 5: Heatmap Display of Pneumonia Detection

This study's results are modeled using the GradCam heatmap technique [59]. The findings of the optimal configuration of the genetic algorithm show a considerable difference in the detection results based on the modeling. The original image of pneumonia with the findings of the heatmap technique, as shown in Figure 5, reveals that the reddish appearance is part of bacterial pneumonia. The non-pneumonic picture, on the other hand, produces a bluish image, indicating that it is not part of the disease-causing

IV. CONCLUSIONS

Rapid test detection of bacterial cells (Acinetobacter baumannii and Pseudomonas aeruginosa) can help identify and screen people with pneumonia. Artificial intelligence methods can be used and applied to assist this process. In this study, one of these methods, namely DenseNet, was used for training to detect pneumonia bacterial cells. The results of the learning accuracy rate reached 95% for DenseNet121 and 96.7% for DenseNet169. Although the resulting accuracy is relatively high, an optimization method using a Genetic Algorithm is applied to obtain maximum results. Therefore, the optimal final result for the two architectures reached 100% accuracy. The highest training model was successfully used as a reference value for a computer-based application to detect pneumonia bacteria with a prediction time of less than 10s.

ACKNOWLEDGMENT

The authors express their sincere gratitude to the Electrical Engineering Study Program of Ahmad Dahlan University for their support in providing computer environment and automation laboratory access. I also thank the School of Nursing Study Program of Universitas Muhammadiyah Yogyakarta for assistance, input, and in-depth reviews of bacteria and hospital nursing.

REFERENCES

[1] L. C. Antunes, P. Visca, and K. J. Towner, "Acinetobacter baumannii: evolution of a global pathogen," *Pathog Dis*, vol. 71, no. 3, pp. 292–301, 2014, doi: 10.1111/2049-632X.12125.

[2] O. Ayobami, N. Willrich, T. Harder, I. N. Okeke, T. Eckmanns, and R. Markwart, "The incidence and prevalence of hospital-acquired (carbapenem-resistant) Acinetobacter baumannii in Europe, Eastern Mediterranean and Africa: a systematic review and meta-analysis," *Emerg Microbes Infect*, vol. 8, no. 1, pp. 1747–1759, 2019, doi: 10.1080/22221751.2019.1698273.

[3] C. L. Holmes, M. T. Anderson, H. L. T. Mobley, and M. A. Bachman, "Pathogenesis of Gram-Negative Bacteremia," *Clin. Microbiol. Rev.*, vol. 34, no. 2, Mar. 2021, doi: 10.1128/CMR.00234-20.

[4] A. Howard, M. O'Donoghue, A. Feeney, and R. D. Sleator, "Acinetobacter baumannii: an emerging opportunistic pathogen," *Virulence*, vol. 3, no. 3, pp. 243–250, 2012, doi: 10.4161/viru.19700.

[5] E. Sharifipour *et al.*, "Evaluation of bacterial co-infections of the respiratory tract in COVID-19 patients admitted to ICU," *BMC Infect Dis*, vol. 20, no. 1, p. 646, 2020, doi: 10.1186/s12879-020-05374-z.

[6] C. Ayoub Moubareck and D. Hammoudi Halat, "Insights into Acinetobacter baumannii: A Review of Microbiological, Virulence, and Resistance Traits in a Threatening Nosocomial Pathogen," *Antibiot.*, vol. 9, no. 3, 2020, doi: 10.3390/antibiotics9030119.

[7] S. S. Jean, Y. C. Chang, W. C. Lin, W. S. Lee, P. R. Hsueh, and C. W. Hsu, "Epidemiology, Treatment, and Prevention of Nosocomial Bacterial Pneumonia," *J Clin Med*, vol. 9, no. 1, 2020, doi: 10.3390/jcm9010275.

[8] S. Mohd Sazlly Lim, A. Zainal Abidin, S. M. Liew, J. A. Roberts, and F. B. Sime, "The global prevalence of multidrug-resistance among Acinetobacter baumannii causing hospital-acquired and ventilator-associated pneumonia and its associated mortality: A systematic review and meta-analysis," *J Infect*, vol. 79, no. 6, pp. 593–600, 2019, doi: 10.1016/j.jinf.2019.09.012.

[9] C. E. Luyt, G. Hekimian, D. Koulenti, and J. Chastre, "Microbial cause of ICU-acquired pneumonia: hospital-acquired pneumonia versus ventilator-associated pneumonia," *Curr Opin Crit Care*, vol. 24, no. 5, pp. 332–338, 2018, doi: 10.1097/MCC.0000000000000526.

[10] R. Zaragoza *et al.*, "Update of the treatment of nosocomial pneumonia in the ICU," *Crit Care*, vol. 24, no. 1, p. 383, 2020, doi: 10.1186/s13054-020-03091-2.

[11] H. S. Sader, M. Castanheira, L. R. Duncan, and R. K. Flamm, "Antimicrobial Susceptibility of Enterobacteriaceae and Pseudomonas aeruginosa Isolates from United States Medical Centers Stratified by Infection Type: Results from the International Network for Optimal Resistance Monitoring (INFORM) Surveillance Program," *Diagn Microbiol Infect Dis*, vol. 92, no. 1, pp. 69–74, 2018, doi: 10.1016/j.diagmicrobio.2018.04.012.

[12] J. P. Horcajada *et al.*, "Epidemiology and Treatment of Multidrug-Resistant and Extensively Drug-Resistant Pseudomonas aeruginosa Infections," *Clin Microbiol Rev*, vol. 32, no. 4, 2019, doi: 10.1128/CMR.00031-19.

[13] X. Chen *et al.*, "The microbial coinfection in COVID-19," *Appl. Microbiol. Biotechnol.*, vol. 104, no. 18, pp. 7777–7785, Sep. 2020, doi: 10.1007/s00253-020-10814-6.

[14] S. Hughes, O. Troise, H. Donaldson, N. Mughal, and L. S. P. Moore, "Bacterial and fungal coinfection among hospitalized patients with COVID-19: a retrospective cohort study in a UK secondary-care setting," *Clin. Microbiol. Infect.*, vol. 26, no. 10, pp. 1395–1399, Oct. 2020, doi: 10.1016/j.cmi.2020.06.025.

[15] G. A. Ospina-Tascón *et al.*, "Effect of High-Flow Oxygen Therapy vs Conventional Oxygen Therapy on Invasive Mechanical Ventilation and Clinical Recovery in Patients With Severe COVID-19," *JAMA*, vol. 326, no. 21, p. 2161, Dec. 2021, doi: 10.1001/jama.2021.20714.

[16] M. E. Ibrahim, "Prevalence of Acinetobacter baumannii in Saudi Arabia: risk factors, antimicrobial resistance patterns and mechanisms of carbapenem resistance," *Ann. Clin. Microbiol. Antimicrob.*, vol. 18, no. 1, p. 1, Dec. 2019, doi: 10.1186/s12941-018-0301-x.

[17] T. Zhang, X. Xu, C.-F. Xu, S. R. Bilya, and W. Xu, "Mechanical ventilation-associated pneumonia caused by Acinetobacter baumannii in Northeast China region: analysis of genotype and drug resistance of bacteria and patients' clinical features over 7 years," *Antimicrob. Resist. Infect. Control*, vol. 10, no. 1, p. 135, Dec. 2021, doi: 10.1186/s13756-021-01005-7.

[18] L. Lansbury, B. Lim, V. Baskaran, and W. S. Lim, "Co-infections in people with COVID-19: a systematic review and meta-analysis," *J Infect*, vol. 81, no. 2, pp. 266–275, 2020, doi: 10.1016/j.jinf.2020.05.046.

[19] C. Garcia-Vidal *et al.*, "Incidence of co-infections and superinfections in hospitalized patients with COVID-19: a retrospective cohort study," *Clin Microbiol Infect*, vol. 27, no. 1, pp. 83–88, 2021, doi: 10.1016/j.cmi.2020.07.041.

[20] F. X. Lescure *et al.*, "Clinical and virological data of the first cases of COVID-19 in Europe: a case series," *Lancet Infect Dis*, vol. 20, no. 6, pp. 697–706, 2020, doi: 10.1016/S1473-3099(20)30200-0.

[21] Y. Deng *et al.*, "Clinical characteristics of fatal

and recovered cases of coronavirus disease 2019 in Wuhan, China: a retrospective study," *Chin Med J*, vol. 133, no. 11, pp. 1261–1267, 2020, doi: 10.1097/CM9.0000000000000824.

[22] L. Wang *et al.*, "Coronavirus disease 2019 in elderly patients: Characteristics and prognostic factors based on 4-week follow-up," *J Infect*, vol. 80, no. 6, pp. 639–645, 2020, doi: 10.1016/j.jinf.2020.03.019.

[23] M. W. Azam and A. U. Khan, "Updates on the pathogenicity status of Pseudomonas aeruginosa," *Drug Discov Today*, vol. 24, no. 1, pp. 350–359, 2019, doi: 10.1016/j.drudis.2018.07.003.

[24] J. Garnacho-Montero and J. F. Timsit, "Managing Acinetobacter baumannii infections," *Curr Opin Infect Dis*, vol. 32, no. 1, pp. 69–76, 2019, doi: 10.1097/QCO.0000000000000518.

[25] H.-G. Wu, W.-S. Liu, M. Zhu, and X.-X. Li, "Research and analysis of 74 bloodstream infection cases of Acinetobacter baumannii and drug resistance.," *Eur. Rev. Med. Pharmacol. Sci.*, vol. 22, no. 6, pp. 1782–1786, Mar. 2018, doi: 10.26355/eurrev_201803_14597.

[26] C. Rodriguez-Lucas *et al.*, "Pseudomonas aeruginosa nosocomial meningitis in neurosurgical patients with intraventricular catheters: Therapeutic approach and review of the literature," *Enferm Infecc Microbiol Clin (Engl Ed)*, vol. 38, no. 2, pp. 54–58, 2020, doi: 10.1016/j.eimc.2019.04.003.

[27] S. Pai *et al.*, "Pseudomonas aeruginosa meningitis/ventriculitis in a UK tertiary referral hospital," *QJM*, vol. 109, no. 2, pp. 85–89, 2016, doi: 10.1093/qjmed/hcv094.

[28] S. Chusri *et al.*, "Outcomes of adjunctive therapy with intrathecal or intraventricular administration of colistin for post-neurosurgical meningitis and ventriculitis due to carbapenem-resistant acinetobacter baumannii," *Int J Antimicrob Agents*, vol. 51, no. 4, pp. 646–650, 2018, doi: 10.1016/j.ijantimicag.2017.12.002.

[29] I. Kyriakidis, E. Vasileiou, Z. D. Pana, and A. Tragiannidis, "Acinetobacter baumannii Antibiotic Resistance Mechanisms," *Pathogens*, vol. 10, no. 3, 2021, doi: 10.3390/pathogens10030373.

[30] D. Wong, T. B. Nielsen, R. A. Bonomo, P. Pantapalangkoor, B. Luna, and B. Spellberg, "Clinical and Pathophysiological Overview of Acinetobacter Infections: a Century of Challenges," *Clin Microbiol Rev*, vol. 30, no. 1, pp. 409–447, 2017, doi: 10.1128/CMR.00058-16.

[31] E. N. Johnson, T. C. Burns, R. A. Hayda, D. R. Hospenthal, and C. K. Murray, "Infectious complications of open type III tibial fractures among combat casualties," *Clin Infect Dis*, vol. 45, no. 4, pp. 409–415, 2007, doi: 10.1086/520029.

[32] M. M. Elmassry *et al.*, "New markers for sepsis caused by Pseudomonas aeruginosa during burn infection," *Metabolomics*, vol. 16, no. 3, p. 40, 2020, doi: 10.1007/s11306-020-01658-2.

[33] J. W. Newman, R. V Floyd, and J. L. Fothergill, "The contribution of Pseudomonas aeruginosa virulence factors and host factors in the establishment of urinary tract infections," *FEMS Microbiol Lett*, vol. 364, no. 15, 2017, doi: 10.1093/femsle/fnx124.

[34] D. Ironmonger, O. Edeghere, A. Bains, R. Loy, N. Woodford, and P. M. Hawkey, "Surveillance of antibiotic susceptibility of urinary tract pathogens for a population of 5.6 million over 4 years," *J Antimicrob Chemother*, vol. 70, no. 6, pp. 1744–1750, 2015, doi: 10.1093/jac/dkv043.

[35] C. T. Chen *et al.*, "Community-acquired bloodstream infections caused by Acinetobacter baumannii: A matched case-control study," *J Microbiol Immunol Infect*, vol. 51, no. 5, pp. 629–635, 2018, doi: 10.1016/j.jmii.2017.02.004.

[36] L. H. Moehario, T. Esterita, V. Shirleen, T. Robertus, and Y. Angelina, "Association of Acinetobacter Baumannii with invasive procedures in hospitalized patients in Jakarta," *J Infect Dev Ctries*, vol. 14, no. 12, pp. 1455–1460, 2020, doi: 10.3855/jidc.12525.

[37] A. Manickam, J. Jiang, Y. Zhou, A. Sagar, R. Soundrapandiyan, and R. Dinesh Jackson Samuel, "Automated pneumonia detection on chest X-ray images: A deep learning approach with different optimizers and transfer learning architectures," *Measurement*, vol. 184, p. 109953, Nov. 2021, doi: 10.1016/j.measurement.2021.109953.

[38] X. Yu, S.-H. Wang, and Y.-D. Zhang, "CGNet: A graph-knowledge embedded convolutional neural network for detection of pneumonia," *Inf. Process. Manag.*, vol. 58, no. 1, p. 102411, Jan. 2021, doi: 10.1016/j.ipm.2020.102411.

[39] S. Motamed, P. Rogalla, and F. Khalvati, "Data augmentation using Generative Adversarial Networks (GANs) for GAN-based detection of Pneumonia and COVID-19 in chest X-ray images," *Informatics Med. Unlocked*, vol. 27, p. 100779, 2021, doi: 10.1016/j.imu.2021.100779.

[40] M. La Salvia *et al.*, "Deep learning and lung ultrasound for Covid-19 pneumonia detection and severity classification," *Comput. Biol. Med.*, vol. 136, p. 104742, Sep. 2021, doi: 10.1016/j.compbiomed.2021.104742.

[41] H. I. K. Fathurrahman, A. Ma'arif, and L.-Y. Chin, "The Development of Real-Time Mobile Garbage Detection Using Deep Learning," *J. Ilm. Tek. Elektro Komput. dan Inform.*, vol. 7, no. 3, p. 472, Jan. 2022, doi: 10.26555/jiteki.v7i3.22295.

[42] A. L. Prasasti, I. A. Rahmi, S. F. Nurahmani, and A. Dinimaharawati, "Mental Health Helper:

Intelligent Mobile Apps in the Pandemic Era," *J. Ilm. Tek. Elektro Komput. dan Inform.*, vol. 7, no. 3, p. 479, Jan. 2022, doi: 10.26555/jiteki.v7i3.22012.

[43] J. G. M. Esgario, P. B. C. de Castro, L. M. Tassis, and R. A. Krohling, "An app to assist farmers in the identification of diseases and pests of coffee leaves using deep learning," *Inf. Process. Agric.*, vol. 9, no. 1, pp. 38–47, Mar. 2022, doi: 10.1016/j.inpa.2021.01.004.

[44] W.-L. Mao, W.-C. Chen, H. I. K. Fathurrahman, and Y.-H. Lin, "Deep learning networks for real-time regional domestic waste detection," *J. Clean. Prod.*, vol. 344, p. 131096, Apr. 2022, doi: 10.1016/j.jclepro.2022.131096.

[45] N. M. DiFilippo and M. K. Jouaneh, "A System Combining Force and Vision Sensing for Automated Screw Removal on Laptops," *IEEE Trans. Autom. Sci. Eng.*, vol. 15, no. 2, pp. 887–895, Apr. 2018, doi: 10.1109/TASE.2017.2679720.

[46] S. K. Tao Hwa, A. Bade, M. H. A. Hijazi, and M. Saffree Jeffree, "Tuberculosis detection using deep learning and contrastenhanced canny edge detected X-Ray images," *IAES Int. J. Artif. Intell.*, vol. 9, no. 4, p. 713, Dec. 2020, doi: 10.11591/ijai.v9.i4.pp713-720.

[47] T. H. Saragih, V. N. Wijayaningrum, and M. Haekal, "Jatropha Curcas Disease Identification using Random Forest," *J. Ilm. Tek. Elektro Komput. dan Inform.*, vol. 7, no. 1, p. 9, Apr. 2021, doi: 10.26555/jiteki.v7i1.20141.

[48] B. Liu *et al.*, "Using deep learning to detect patients at risk for prostate cancer despite benign biopsies," *iScience*, vol. 25, no. 7, p. 104663, Jul. 2022, doi: 10.1016/j.isci.2022.104663.

[49] P. Purwono, A. Ma'arif, I. S. Mangku Negara, W. Rahmaniar, and J. Rahmawan, "Linkage Detection of Features that Cause Stroke using Feyn Qlattice Machine Learning Model," *J. Ilm. Tek. Elektro Komput. dan Inform.*, vol. 7, no. 3, p. 423, Dec. 2021, doi: 10.26555/jiteki.v7i3.22237.

[50] S. Alghyaline, "Real-time Jordanian license plate recognition using deep learning," *J. King Saud Univ. - Comput. Inf. Sci.*, vol. 34, no. 6, pp. 2601–2609, Jun. 2022, doi: 10.1016/j.jksuci.2020.09.018.

[51] J. G. Choi, C. W. Kong, G. Kim, and S. Lim, "Car crash detection using ensemble deep learning and multimodal data from dashboard cameras," *Expert Syst. Appl.*, vol. 183, p. 115400, Nov. 2021, doi: 10.1016/j.eswa.2021.115400.

[52] I. Ihsan, E. W. Hidayat, and A. Rahmatulloh, "Identification of Bacterial Leaf Blight and Brown Spot Disease In Rice Plants With Image Processing Approach," *J. Ilm. Tek. Elektro Komput. dan Inform.*, vol. 5, no. 2, p. 59, Feb. 2020, doi: 10.26555/jiteki.v5i2.14136.

[53] T. Li *et al.*, "An improved binocular localization method for apple based on fruit detection using deep learning," *Inf. Process. Agric.*, Dec. 2021, doi: 10.1016/j.inpa.2021.12.003.

[54] M. D. Fauzi, F. Dharma Adhinata, N. G. Ramadhan, N. Annisa, and F. Tanjung, "A Hybrid DenseNet201-SVM for Robust Weed and Potato Plant Classification," *J. Ilm. Tek. Elektro Komput. dan Inform.*, vol. 8, no. 2, pp. 298–306, 2022, doi: 10.26555/jiteki.v8i2.23886.

[55] B. Zieliński, A. Plichta, K. Misztal, P. Spurek, M. Brzychczy-Włoch, and D. Ochońska, "Deep learning approach to bacterial colony classification," *PLoS One*, vol. 12, no. 9, p. e0184554, Sep. 2017, doi: 10.1371/journal.pone.0184554.

[56] W. L. Mao, H. I. K. Fathurrahman, Y. Lee, and T. W. Chang, "EEG dataset classification using CNN method," in *Journal of physics: conference series*, 2020, vol. 1456, no. 1, p. 12017.

[57] F. Gama, A. G. Marques, G. Leus, and A. Ribeiro, "Convolutional Neural Network Architectures for Signals Supported on Graphs," *IEEE Trans. Signal Process.*, vol. 67, no. 4, pp. 1034–1049, 2019, doi: 10.1109/TSP.2018.2887403.

[58] D. P. Brogan, N. M. DiFilippo, and M. K. Jouaneh, "Deep learning computer vision for robotic disassembly and servicing applications," *Array*, vol. 12, p. 100094, Dec. 2021, doi: 10.1016/j.array.2021.100094.

[59] R. R. Selvaraju, M. Cogswell, A. Das, R. Vedantam, D. Parikh, and D. Batra, "Grad-CAM: Visual Explanations from Deep Networks via Gradient-Based Localization," *Int. J. Comput. Vis.*, vol. 128, no. 2, pp. 336–359, 2020, doi: 10.1007/s11263-019-01228-7.